GSA DATA REPOSITORY 2015183

What makes a delta wave-dominated?

Jaap H. Nienhuis, Andrew D. Ashton, Liviu Giosan

Supplemental Methods

Alongshore sediment transport is computed using the CERC or Komar (Komar, 1998) formula, reformulated into deep-water wave properties (Ashton and Murray, 2006) by back-refracting the waves over shore-parallel contours, which yields:

$$Q_s = K_1 \cdot \rho_s \cdot (1-p) \cdot H_s^{12/5} T^{1/5} \cos^{6/5}(\phi_0 - \theta)\sin(\phi_0 - \theta), \quad (1)$$

in units of kgs^{-1}. Where

$$K_1 = 5.3 \cdot 10^{-6} \cdot K \left(\frac{1}{2n}\right)^{6/5} \left(\frac{\sqrt{g\gamma_b}}{2\pi}\right)^{1/5}, \quad (2)$$

is an empirical constant that equals ~ 0.06 m$^{3/5}$s$^{-6/5}$. $K = 0.46\rho g^{3/2}$ (Komar, 1998), H_s is the offshore deep-water significant wave height (m), T is the wave period (s), ϕ_0 is the deep-water wave approach angle, and θ is the local shoreline orientation (Ashton and Murray, 2006) (Fig. 1c). The density of water and sediment are denoted by ρ and ρ_s (kgm^{-3}), p is the dry mass void fraction, g is the gravitational acceleration (ms^{-2}), γ_b is the ratio of breaking wave height and water depth (γ_b = 0.78), and n is the ratio of group velocity to phase velocity of the breaking waves (1 in shallow water). With the angles defined as in figure 1a, Q_s is positive to the right looking offshore.

As waves approach the shore from different angles over time, they contribute to Q_s either to the left or the right. Integrated over time, the relative contribution of each wave direction to the alongshore sediment transport is given by the wave energy probability density distribution (Fig. 1b),

$$E(\phi_0) = \frac{H_s^{12/5}(\phi_0) \cdot T^{1/5}(\phi_0)}{\sum_{\phi_0} H_s^{12/5}(\phi_0) \cdot T^{1/5}(\phi_0)} . \tag{3}$$

The net alongshore sediment transport for a shoreline orientation θ is therefore given by the convolution integral of the wave energy probability distribution E and the alongshore sediment transport function Q_s,

$$Q_{s,net}(\theta) = E(\phi_0) * Q_s(\phi_0 - \theta), \tag{4}$$

with Q_s as defined in equation (1) (Fig. 1d). The deep-water significant wave height is $H_{s,net} = \left(\frac{1}{N} \sum_N H_s^{12/5} \right)^{5/12}$ and the wave period is $T_{net} = \left(\frac{1}{N} \sum_N T^{1/5} \right)^5$.

The maximum alongshore littoral transport away from the river mouth $Q_{s,max}(\theta)$ is the sum of the maximum fluxes to the left and right delta flank,

$$Q_{s,\max} = Q_{s,\max,r} - Q_{s,\max,l}, \tag{5}$$

$$Q_{s,\max} = \max_{-\pi \le \theta \le 0} \left[E(\phi_0) * Q_{s,r}(\phi_0 - \theta) \right] - \min_{0 \le \theta \le \pi} \left[E(\phi_0) * Q_{s,l}(\phi_0 - \theta) \right] . \tag{6}$$

Note that the minus sign and the minimum function arise from the definition of Q_s, being positive to the right looking offshore.

For the drainage basins in Java, we compute sediment discharge using the BQART formula (Syvitski and Milliman, 2007), which estimates fluvial sediment flux based upon drainage area, basin climate, and relief,

$$Q_r = \omega B Q^{0.31} A^{0.5} R T \quad (7)$$

where ω=0.02 is a fitting parameter, $B = IL\,(1-T_E)E_h$ accounts for geologic and land use factors, Q is the fluvial water discharge (m^3s^{-1}), A is the drainage basin area (km^2), R is the relief (elevation maximum, km) and T is the basin average temperature (°C). For B, I is a glacial erosion factor (1 in this case) and L captures the soil erodibility. T_E and E_h account respectively for the anthropogenic trapping of sediment and increase in soil erosion, which we assume to cancel out (Syvitski and Milliman, 2007). Drainage basin areas and relief are retrieved from the USGS HydroSHEDS database (Lehner et al., 2008). Supplementary Tables 1 and 2 list the values used in this study. Based on estimates on the sand fraction in the Porong river in East-Java (Hoekstra, 1989), we assume that 10% (the sand or littoral grade fraction) of the total fluvial sediment flux ($Q_{r,total}$) directly amalgamates to the shoreline.

We measure shoreline orientation θ close to the river mouth of the left and right flanks of every delta, and the orientation of the non-deltaic coastline. As the Java deltas are generally symmetrical or close to it, we use an average of the two shoreline angles as a representative transport angle. To estimate wave climatology, we use the NOAA WaveWatch III hindcast reanalysis data of 1997 to 2010 (Chawla et al., 2011).

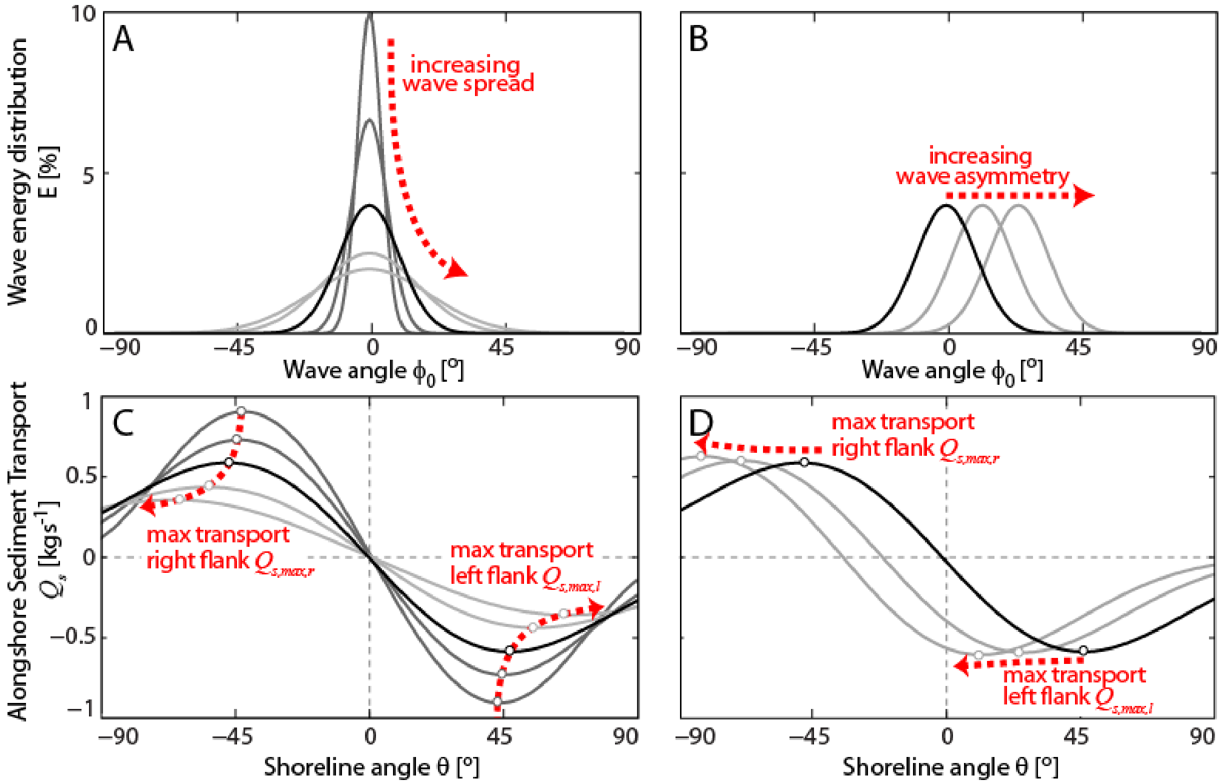

Supplementary Figure 1. Effect of wave climate distribution on θ_{max} and $Q_{s,max}$. Hypothetical wave distributions with varying (A) wave angle spread and (B) mean approach angle with (C, D) corresponding littoral transport as a function of shoreline orientation for the wave climates in the upper panels, normalized to Q_s at zero standard deviation. Red dotted lines track the location of the maxima for changes in the wave distribution.

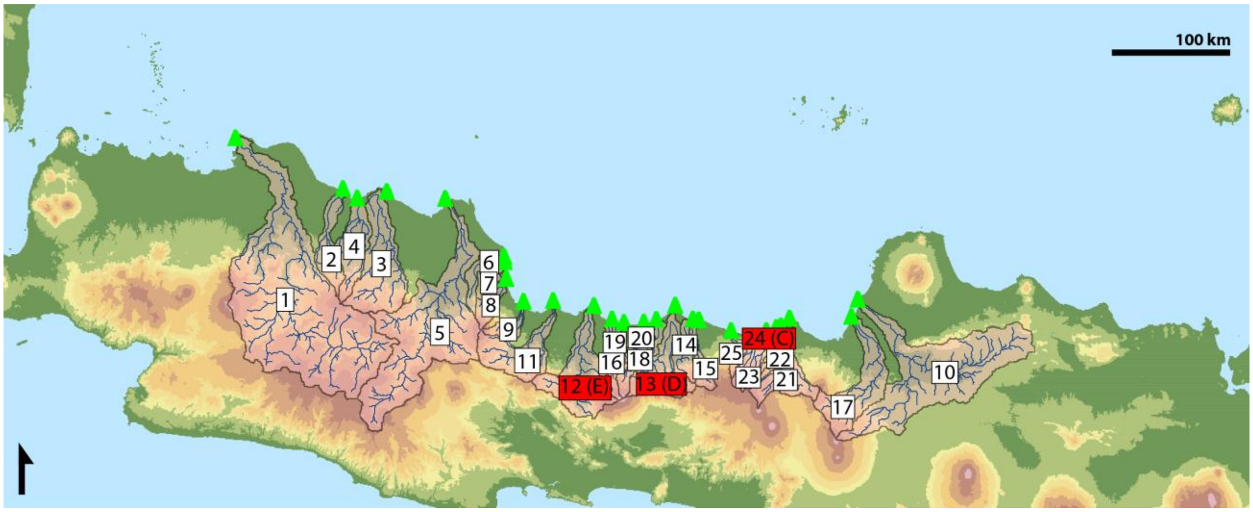

Supplementary Figure 2. Drainage basins of 25 deltas and the subaerial elevation from SRTM data (Farr and Kobrick, 2000). Red markers correspond to the examples displayed in Figure 2. See Supplementary Table 1.

Supplementary Table 1: Morphologic and drainage basin properties of deltas along the Java, Indonesia, coastline. The index # corresponds to the numbers in Supplementary Figure 2. The names of rivers 2, 9, 11, 19 and 22 are unknown to the authors. (*) indicates that the deltaic shoreline is visually river-dominated and therefore the shoreline orientation is unmeasurable.

#	River	Lat	Lon	Drainage Area *A* [km^2]	Relief *R* [km]	Water Flux *Q* [km^{3}yr^{-1}]	Sediment Flux $Q_{r,total}$ [kgs^{-1}]	Shoreline angle [°]	Left flank angle, θ_l[°]	Right flank angle, θ_r [°]	Average flank angle θ [°]	Max Littoral Transport $Q_{s,max}$ [kgs^{-1}]	Fluvial Dominance R
1	Citarum/Sungai	-5.939	107.010	6709	2.964	86	1122	246	*	*	*	47	2.40
2	?	-6.194	107.623	548	1.764	12	103	297	270	143	26.5	22	0.47
3	Kali Pontjol	-6.208	107.874	1442	2.036	25	244	306	*	*	*	28	0.87
4	Tji Asem	-6.242	107.706	730	2.051	15	148	262	229	115	33	23	0.64
5	Cimanuk	-6.242	108.207	3692	2.886	54	699	240	*	*	*	16	4.33
6	Kali Pondok	-6.536	108.544	273	0.641	7	22	347	342	172	5	48	0.05
7	Waringin	-6.561	108.545	197	0.385	5	10	362	350	193	11.5	52	0.02
8	Kali Truivag	-6.646	108.557	274	2.967	7	103	355	337	192	17.5	50	0.21
9	?	-6.759	108.656	213	2.866	5	82	268	225	131	43	22	0.38
10	Serang River	-6.749	110.563	3424	2.806	50	642	212	*	*	*	30	2.14
11	?	-6.756	108.825	925	2.965	18	255	278	227	148	50.5	26	0.98
12	Sungai pemali	-6.781	109.058	1334	2.569	24	290	278	*	*	*	18	1.64
13	Kali Tjomal	-6.780	109.521	817	2.803	16	220	276	227	145	49	26	0.83
14	Kali Sragi	-6.848	109.622	322	1.185	8	46	282	271	112	10.5	26	0.18
15	Kali Baro	-6.853	109.657	265	1.907	7	64	285	272	117	12.5	26	0.25
16	Danawari	-6.848	109.160	226	3.319	6	99	282	262	122	20	27	0.37
17	Kali Tuntang	-6.836	110.527	1171	3.004	21	308	200	144	76	56	47	0.65
18	Kali Labon	-6.852	109.415	291	3.376	7	122	250	249	71	1	26	0.47
19	?	-6.866	109.230	155	0.586	4	13	275	262	108	13	27	0.05
20	Kali Brungut	-6.864	109.342	229	0.726	6	22	261	251	91	10	27	0.08
21	Bodri	-6.844	110.174	626	2.512	13	161	268	225	130	42.5	50	0.32
22	?	-6.882	110.124	153	1.358	4	30	246	244	67	1.5	49	0.06
23	Kali Blukar	-6.892	110.098	395	1.595	9	72	253	249	76	3.5	40	0.18
24	Kali Satrian	-6.907	110.042	106	2.524	3	43	257	244	90	13	26	0.16
25	Kali Ambo	-6.907	109.841	128	1.672	4	33	280	275	105	5	26	0.13

Supplementary Table 2: BQART factors and their values and references as used in this study.

Variable	Value	Note [units]	Reference
$Q_{r,total}$		Estimated total fluvial sediment flux: $Q_{r,total} = \omega B Q^{0.31} A^{0.5} R T$ [kgs^{-1}]	(Syvitski and Milliman, 2007)
ω	0.02	Fitting parameter [$kgs^{-0.69} km^{-2} °C^{-1} m^{-0.93}$]	(Syvitski and Milliman, 2007)
B	2	Accumulated geologic and land use factors: $B = I\,L(1-T_E)E_h$ [-]	(Syvitski and Milliman, 2007)
Q		Fluvial water discharge, $Q=0.075A^{0.8}$ [m^3s^{-1}]	(Syvitski and Milliman, 2007)
A		Drainage basin area, retrieved from USGS HydroSHEDS [km^2]	(Lehner et al., 2008)
R		Relief (maximum elevation) retrieved from SRTM 15s DEM data [km]	(Farr and Kobrick, 2000)
T	28	Basin-wide average temperature [°C]	(World Meteorological Organization, 2014)
I	1	Glacial erosion factor [-]	
L	2	Soil erodibility [-]	(Syvitski and Milliman, 2007)
T_E		Anthropogenic trapping of sediment, we assume no net anthropogenic effect [-]	
E_h		Anthropogenic increase in soil erosion, we assume no net anthropogenic effect [-]	

Supplementary Table 3: Properties and flux estimates for 4 well-documented deltas. (*) indicates that the deltaic shoreline is river-dominated and therefore the shoreline orientation is unmeasurable. We assume a sand fraction of 10% for the Senegal and the Sao Francisco rivers.

Delta	**Lat**	**Lon**	**Fluvial sand flux Q_r [kgs^{-1}]**	**Shoreline Angle [°]**	**Left Flank Angle, θ_l [°]**	**Right Flank Angle, θ_r [°]**	**Average flank angle θ [°]**	**Max Littoral Transport $Q_{s,max}$ [kgs^{-1}]**	**Fluvial Dominance *R***	**Ref**
Senegal	15.99	-16.51	15	184	0	3	2	225	0.04	(Martins and Probst, 1991; Chawla et al., 2011)
Sao Francisco	-10.48	-36.40	75	50	21	22	22	280	0.3	(Lima et al., 2005; Chawla et al., 2011)
Tinajones, Sinu	9.420	-75.92	133	247	*	*	*	65	2	(Restrepo et al., 2009; Chawla et al., 2011)
Belize, Mississippi	29.20	-89.30	919	82	*	*	*	130	7	(Chawla et al., 2011; Nittrouer and Viparelli, 2014)

References

Ashton, A.D., and Murray, A.B., 2006, High-angle wave instability and emergent shoreline shapes: 1. Modeling of sand waves, flying spits, and capes: Journal of Geophysical Research, v. 111, no. F4, p. F04011, doi: 10.1029/2005JF000422.

Chawla, A., Spindler, D., and Tolman, H.L., 2011, A Thirty Year Wave Hindcast Using The Latest NCEP Climate Forecast System Reanalysis Winds, *in* Proceedings of the 12th International Workshop on Wave Hindcasting and Forecasting, Kohala Coast, Hawaii.

Farr, T.G., and Kobrick, M., 2000, Shuttle radar topography mission produces a wealth of data: Eos, Transactions American Geophysical Union, v. 81, no. 48, p. 583, doi: 10.1029/EO081i048p00583.

Hoekstra, P., 1989, Hydrodynamics and depositional processes of the Solo and Porong Deltas, East Java, Indonesia, *in* Linden, W.J.M. van der, Cloetingh, S.A.P.L., Kaasschieter, J.P.., Graaff, W.J.. van de, Vandenberghe, J., and Gun, J.A.M. van der eds., Proceedings KNGMG Symposium “Coastal Lowlands, Geology and Geotechnology,” Springer Science+Business Media, Dordrecht, p. 161–173.

Komar, P.D., 1998, Beach processes and sedimentation: Prentice Hall, Upper Saddle River, NJ. 544 p.

Lehner, B., Verdin, K., and Jarvis, A., 2008, New Global Hydrography Derived From Spaceborne Elevation Data: Eos, Transactions American Geophysical Union, v. 89, no. 10, p. 93, doi: 10.1029/2008EO100001.

Lima, J.E.F.W., Lopes, W.T.A., De Oliveira Carvalho, N., Vieira, M.R., and Da Silva, E.M., 2005, Suspended sediment fluxes in the large river basins of Brazil, *in* Walling, D.E. and Horowitz, A.J. eds., IAHS ICCE symposium: Sediments Budgets 1, IAHS Publications, p. 355–364.

Martins, O., and Probst, J.-L., 1991, Biogeochemistry of Major African Rivers: Carbon and Mineral Transport, *in* Degens, E.T., Kempe, S., and Richley, J.E. eds., Biogeochemistry of Major World Rivers, John Wiley & Sons, Ltd., p. 127–155.

Nittrouer, J.A., and Viparelli, E., 2014, Sand as a stable and sustainable resource for nourishing the Mississippi River delta: Nature Geoscience, v. 7, no. 5, p. 350–354, doi: 10.1038/ngeo2142.

Restrepo, J.D., López, S.A., and Restrepo, J.C., 2009, The effects of geomorphic controls on sediment yield in the Andean rivers of Colombia: Latin American Journal of Sedimentology and Basin analysis, v. 16, no. 2, p. 79–92.

Syvitski, J.P.M., and Milliman, J.D., 2007, Geology, Geography, and Humans Battle for Dominance over the Delivery of Fluvial Sediment to the Coastal Ocean: The Journal of Geology, v. 115, no. 1, p. 1–19, doi: 10.1086/509246.

World Meteorological Organization, 2014, WMO Mean Annual Temperature: World Weather: Jakarta, Indonesia, p. http://worldweather.wmo.int/en/city.html?cityId=31.